System-size and energy dependence of particle momentum spectra: The UrQMD analysis of p+p and Pb+Pb collisions

V. Yu. Vovchenko,[1,2,3] D. V. Anchishkin,[4,1] and M. I. Gorenstein[4,2]

[1] *Taras Shevchenko National University of Kiev, Kiev, Ukraine*

[2] *Frankfurt Institute for Advanced Studies, Frankfurt, Germany*

[3] *Goethe University, Frankfurt, Germany*

[4] *Bogolyubov Institute for Theoretical Physics, Kiev, Ukraine*

(Dated: August 15, 2014)

arXiv:1407.0629v2 [nucl-th] 14 Aug 2014

Abstract

The UrQMD transport model is used to study a system-size and energy dependence of the pion production in high energy collisions. New data of the NA61/SHINE Collaboration on spectra of negatively charged pions in proton-proton interactions at SPS energies are considered. These results are compared with the corresponding data of the NA49 Collaboration in central Pb+Pb collisions at the same collision energies per nucleon. Mean pion multiplicity per participant nucleon, inverse slope parameter of the transverse momentum spectra, and width of rapidity distribution are investigated. A role of isospin effects is discussed. We find that the UrQMD model predicts a non-monotonous behavior of mean transverse mass with collision energy for positively charged pions at the mid-rapidity in inelastic proton-proton interactions. This will be checked soon experimentally by NA61/SHINE Collaboration.

PACS numbers: 25.75.Gz, 25.75.Ag

Keywords:

I. INTRODUCTION

During the period of 1999-2002, experimental data on hadron production in Pb+Pb collisions at $p_{\rm lab}$ =20A, 30A, 40A, 80A, and 158A GeV/c were recorded by the NA49 Collaboration at the Super Proton Synchrotron (SPS) of the European Organization for Nuclear Research (CERN) [1–3]. These results are consistent with the onset of deconfinement in central Pb+Pb collisions at about 30A GeV/c [4]. A further progress in understanding the effects related to the onset of deconfinement can be achieved by a new comprehensive study of hadron production in proton-proton, proton-nucleus, and nucleus-nucleus collisions. This motivated the present NA61/SHINE ion programme at the SPS CERN devoted to the system size and energy scan [5, 6]. In parallel to the NA61/SHINE programme the Beam Energy Scan (BES) Programme at the BNL RHIC was proposed [7]. Both programmes were motivated by the NA49 results on the onset of deconfinement and the possibility to observe the critical point of strongly interacting matter. These efforts will be extended by the future Compressed Baryonic Matter (CBM) experiment at the Facility for Antiproton and Ion Research (FAIR) [8]. It employs high intensity beams and large acceptance detectors, and will make it possible to measure rare probes – multi-strange hyperons and open charmed mesons – in proton-proton, proton-nucleus, and nucleus-nucleus collisions. The CBM experiment [9] is expected to start data taking with the beams up to 11A GeV from SIS100 in 2018. A considered addition of SIS300 would increase the energy range to 35A GeV after 2025.

Recently, the NA61/SHINE Collaboration published data [10] on spectra of negatively charged pions produced in inelastic proton-proton (p+p) interactions at $p_{\rm lab}$ = 20, 31, 40, 80, and 158 GeV/c. This is the first experimental step of the system-size scan of NA61/SHINE. Data on ^{7}Be+^{9}Be collisions are already recorded, collisions of Ar+Ca and Xe+La are planned to be registered in 2015 and 2017, respectively.

In the present study the spectra of negatively charged pions in inelastic p+p collisions are considered, and a comparison with the corresponding data on central Pb+Pb collisions is performed. We analyze changes between p+p and Pb+Pb collisions with regards to different hadron observables found in experimental data and compare them to those predicted by theoretical modeling, which is based on the ultra-relativistic quantum molecular dynamics

(UrQMD-3.3p2) model [11, 12]. In the present analysis we use the cascade version of UrQMD without an intermediate hydro stage. The energy dependence of main characteristics of pion spectra are investigated. It is shown that a proper treatment of isospin effects is important for comparison of pion production data in proton-proton and nucleus-nucleus collisions.

The paper is organized as follows. In Sec. II pion multiplicities per participant nucleon are considered. The isospin effects are also discussed. In Sec. III the UrQMD model is used to calculate energy loss of colliding nucleons in inelastic p+p and central nucleus-nucleus collisions. In Sec. IV spectra of π^- mesons produced in inelastic p+p and central Pb+Pb collisions are compared and analyzed with the UrQMD model. A summary in Sec. V closes the article.

II. PION MULTIPLICITIES AND ISOSPIN EFFECTS

Mean multiplicity of pions per participant nucleon as well as properly normalized pion spectra are quite similar in inelastic proton-proton and nucleus-nucleus collisions at the same collision energy per nucleon in the SPS energy range. Therefore, one needs comprehensive data at the same collision energies per nucleon to make a systematic comparison of the pion spectra in p+p and nucleus-nucleus collisions and reveal the physical differences between them. The recent NA61/SHINE data on p+p interactions [10] and the data of NA49 on Pb+Pb collisions [1–3] will be used in the present analysis.

Similar behavior of the pion spectra in proton-proton and nucleus-nucleus collisions explains also a particular vitality of the wounded nucleon model (WNM) [13] which treats the final state in nucleus-nucleus collision as the result of independent particle production from wounded (participant) nucleons. Meanwhile, the WNM model failed to explain the production of strange hadrons and anti-baryons: for these secondary particles a strong difference is observed between proton-proton and nucleus-nucleus collisions.

The UrQMD model will be used for our analysis with event statistics of about $2 \cdot 10^6$ inelastic p+p reactions and $5 \cdot 10^4$ central Pb+Pb collisions. For Pb+Pb collisions the experimental centrality selection is 7.2% at $p_{\rm lab}$ =20A, 30A, 40A, 80A GeV/c and 5% at $p_{\rm lab}$ = 158A GeV/c. In the UrQMD simulations these samplings correspond to the restrictions on the impact parameter $b < 4$ fm and $b < 3.4$ fm, respectively. In fixed target experiments, the centrality

selection is made using the number of projectile spectators measured by a zero degree calorimeter. However, for the first moments, such as the mean number of some particle species, any centrality criteria appears to be equivalent to the geometrical one treated with a help of the impact parameter b [14]. This is not valid for the studies of event-by-event fluctuations (see, e.g., Ref. [15]).

The experimental results for mean number of negatively charged pions $\langle \pi^- \rangle$ divided by average number of participant nucleons $\langle N_p \rangle$ (equal to two for p+p collisions) are shown in Fig. 1. In this figure the energy measure $F = \left(\sqrt{s_{NN}} - 2m_N\right)^{3/4} / \left(\sqrt{s_{NN}}\right)^{1/4}$ is used, where $\sqrt{s_{NN}}$ is the center of mass energy of the nucleon pair and m_N is the nucleon mass. The laboratory energy per nucleon is equal to $E_{\rm lab}/{\rm A} = (s_{NN} - 2m_N^2)/2m_N$. From Fig. 1 it is seen that the quantity $\langle \pi^- \rangle / \langle N_p \rangle$ in central Pb+Pb collisions is larger than in inelastic p+p collisions at all SPS energies. The lines correspond to the UrQMD results. The UrQMD result for inelastic p+p interactions shows a good agreement with the data for the top SPS energies (80 and 158 GeV) but underestimates the experimental values of $\langle \pi^- \rangle / \langle N_p \rangle$ at the lower ones.

To make an accurate comparison of mean pion multiplicities and some other quantities in proton-proton and nucleus-nucleus collisions, one needs to take into account the isospin effects. In nucleus-nucleus reaction, different types of nucleon-nucleon (NN) collisions take place: p+p, p+n, and n+n. The π^- and π^+ multiplicities in inelastic p+p, p+n, and n+n collisions calculated at the SPS energies within the UrQMD model are presented in Fig. 2. The differences between the π^- or π^+ multiplicities in different types of N+N collisions are approximately constant. Thus, the largest relative isospin effects are evidently expected at smallest energies where the absolute values of the pion multiplicities are small.

Let us consider A+A collision as a set of p+p, proton-neutron (p+n), and neutron-neutron (n+n) reactions. Their partial contributions to hadron production in A+A collision will depend on the atomic number A and electric charge Z of colliding nuclei. Hadron multiplicities in N+N reaction will be defined as an appropriate average over all possible p+p, p+n, and n+n collisions taking place in A+A reaction, e.g., for π^i multiplicity ($i = +, -, 0$) one obtains:

$$\langle \pi^i_{NN} \rangle \;=\; \alpha_{pp} \, \langle \pi^i_{pp} \rangle \;+\; \alpha_{pn} \, \langle \pi^i_{pn} \rangle \;+\; \alpha_{nn} \, \langle \pi^i_{nn} \rangle \,, \qquad (1)$$

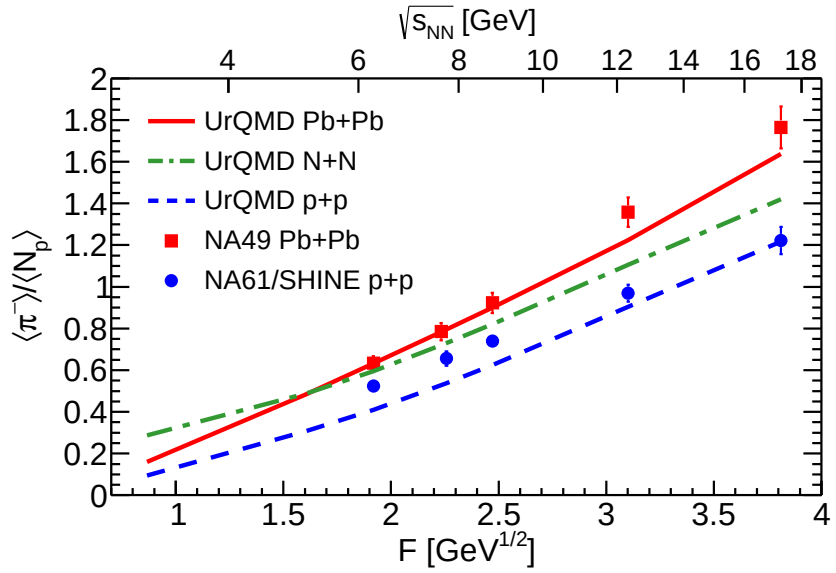

Figure 1: (Color online) Energy dependence of mean π^- multiplicity divided by the average number of participant nucleons. The data of NA49 on central Pb+Pb collisions and NA61/SHINE on inelastic p+p interactions are depicted by symbols. The lines correspond to the UrQMD predictions for inelastic p+p (dashed), central Pb+Pb (solid), and inelastic N+N (dashed-dotted) collisions.

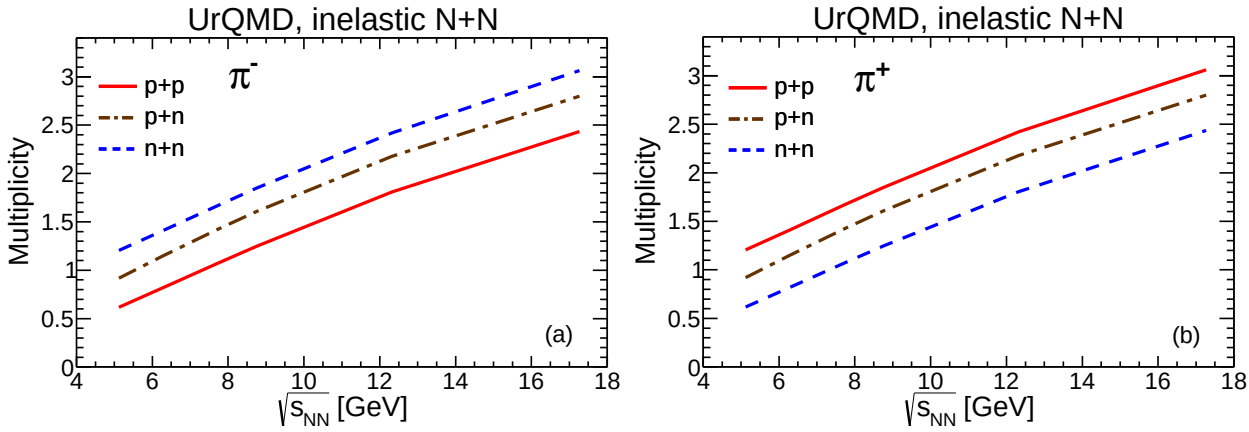

Figure 2: (Color online) Collision energy dependence of mean multiplicity of (a) π^- and (b) π^+ mesons in inelastic p+p, p+n and n+n interactions at SPS energies calculated in the UrQMD model.

where $\alpha_{pp} = Z^2/A^2$, $\alpha_{pn} = 2(A-Z)Z/A^2$, and $\alpha_{nn} = (A-Z)^2/A^2$ are the combinatoric probabilities of p+p, p+n, and n+n collisions, respectively. For light and intermediate nuclei, $Z \cong 0.5A$, whereas for heavy ones, $Z \cong 0.4A$. Therefore, $\alpha_{pp} \cong 0.16$, $\alpha_{pn} \cong 0.48$, and

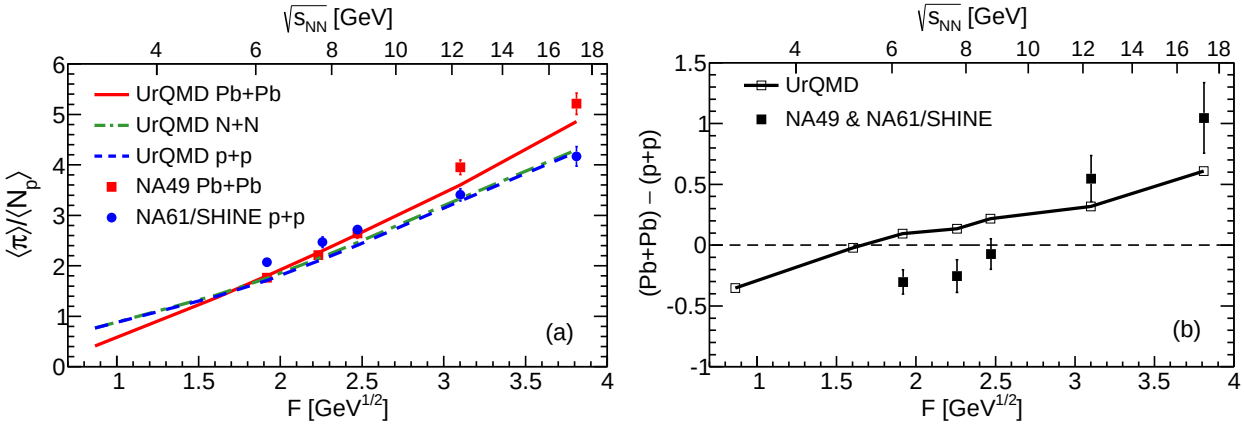

Figure 3: (Color online) (a) The same as in Fig. 1 but for mean multiplicity of all pions. (b) The difference of the mean pion multiplicity per nucleon participant in central Pb+Pb and inelastic p+p collisions. The full symbols correspond to the data of NA49 and NA61/SHINE collaborations. The open symbols connected by solid line show the UrQMD results.

$\alpha_{nn} \cong 0.36$ for Pb+Pb collisions, and $\alpha_{pp} \cong \alpha_{nn} \cong 0.25$ and $\alpha_{nn} \cong 0.5$ in collisions of light and intermediate nuclei. It is clear that relative importance of n+n reactions in A+A collisions increases with atomic number. To avoid a misunderstanding let us stress again that the notion of N+N reaction in Eq. (1) leads to different N+N results for different colliding nuclei.

The behavior of $\langle \pi^-_{NN} \rangle/2$, which is a mean multiplicity of π^- mesons per participant nucleon in a fictitious N+N collision, calculated in UrQMD with Eq. (1) is shown in Fig. 1 by the dashed-dotted line. From this figure, one concludes that an essential part of the difference in $\langle \pi^- \rangle/\langle N_p \rangle$ for p+p and Pb+Pb collisions comes from the isospin effects.

The results of UrQMD calculations for mean multiplicity of all pions divided by the mean number of participant nucleons are shown in Fig. 3a. These results are compared to experimental data from Ref. [10]. The mean multiplicity of all pions is calculated in UrQMD directly as $\langle \pi \rangle = \langle \pi^+ \rangle + \langle \pi^0 \rangle + \langle \pi^- \rangle$. The experimental estimate of the mean pion multiplicity is calculated in accordance with the formula

$$\langle \pi \rangle \;=\; \frac{3}{2}\left(\langle \pi^+ \rangle \;+\; \langle \pi^- \rangle \right) . \qquad (2)$$

It assumes $\langle \pi^0 \rangle = 0.5\,(\langle \pi^+ \rangle + \langle \pi^- \rangle)$ for the mean multiplicity of neutral pions. Both $\langle \pi^+ \rangle$ and $\langle \pi^- \rangle$ were measured in Pb+Pb central collisions. However, no systematic data for $\langle \pi^+ \rangle$ in p+p

reactions are now available. Thus, to construct experimental estimate of $\langle\pi\rangle$ in p+p reactions, Eq. (2) has been supplemented in Ref. [10] by an approximate relation $\langle\pi^+\rangle \cong \langle\pi^-\rangle + 2/3$ [16]. This relation appears to be also approximately valid for the UrQMD results. However, we do not need it in our UrQMD modeling. The UrQMD results for $\langle\pi^+\rangle$, $\langle\pi^0\rangle$, $\langle\pi^-\rangle$ in p+p, p+n, and n+n reactions are used to construct $\langle\pi\rangle$ in p+p and N+N collisions. Both UrQMD values for the mean pion multiplicity – in p+p and N+N reactions – are shown in Fig 3.

The mean pion multiplicity per participant nucleon is larger in inelastic p+p interactions than that in central Pb+Pb collisions at small SPS energies. A possible explanation of the pion suppression in A+A collisions at small energies were discussed in Ref. [17], where the system of pions, nucleons, and deltas were considered. When the system created in A+A collisions evolves towards chemical equilibrium, the initial surplus of deltas created at the early stage of A+A reaction in p+p, n+n, and n+n collisions has to be reduced. The microscopic process responsible for the Δ absorption is $\Delta + N \to N + N$ and is included in UrQMD. This causes the suppression of the final state pions.

The difference between the $\langle\pi\rangle/\langle N_p\rangle$ data values in Pb+Pb and p+p collisions increases with collision energy and changes sign (becomes positive) at about $E_{lab} \approx 40A$ GeV as shown in Fig. 3b. This *kink* in the difference of pion multiplicities per participant nucleon in Pb+Pb and p+p collisions was predicted by the Statistical Model of the Early Stage [4] as the consequence of the onset of deconfinement. As seen from Fig. 3 the UrQMD results also show this type of behavior. However, the difference changes sign at significantly lower energy of about $E_{lab} \approx 10A$ GeV instead of $40A$ GeV.

III. ENERGY LOSS OF COLLIDING NUCLEONS

We introduce the quantity $K_{\rm loss}$ which shows a fraction of the initial kinetic energy lost by each nucleon from the colliding systems to create new secondary particles. In the center of mass system of colliding protons or nucleus this energy loss is defined as

$$K_{\rm loss} \;=\; \frac{\sqrt{s_{_{NN}}}/2 - (\langle E_B\rangle \;-\; \langle E_{\overline{B}}\rangle)/\langle N_p\rangle}{\sqrt{s_{_{NN}}}/2 - m_N} \tag{3}$$

where $\langle E_B\rangle$ and $\langle E_{\overline{B}}\rangle$ are the average values of the energies of baryons and anti-baryons, respectively, in the final state (the nucleon spectators in nucleus-nucleus collisions are excluded)

and $\sqrt{s_{NN}}/2$ is the center of mass energy of a nucleon in the colliding nuclei.

The momentum spectra of baryons and anti-baryons were not yet presented in p+p collisions by NA61. Therefore, one can only rely on the model estimates. The quantity $K_{\rm loss}$ calculated within the UrQMD simulations for inelastic p+p and central Pb+Pb collisions is shown in Fig. 4a. It is seen that, for Pb+Pb collisions, $K_{\rm loss}$ increases with collision energy. This is consistent with data of NA49 on inelasticity K [18], which is a very closely related quantity and is depicted by triangular symbols in Fig. 4a. The UrQMD results demonstrate that at $E_{\rm lab} \geq 20$A GeV the following inequality holds

$$K_{\rm loss}({\rm p+p}) \ < \ K_{\rm loss}({\rm Pb+Pb}) \ , \tag{4}$$

i.e., each nucleon in Pb+Pb collisions transforms more initial kinetic energy to the production of new particles than that in p+p inelastic collisions at the same initial energy per participant nucleon, $\sqrt{s_{NN}}/2$. As seen from Fig. 3, the relation (4) is correlated with the inequality for the total pion multiplicity per participant nucleon

$$\left(\frac{\langle\pi\rangle}{\langle N_p\rangle}\right)_{p+p} \ < \ \left(\frac{\langle\pi\rangle}{\langle N_p\rangle}\right)_{Pb+Pb} \ . \tag{5}$$

To study the dependence of energy loss (3) on the system size we calculate its UrQMD values in central (impact parameter $b = 0$) nucleus-nucleus collisions at different mass number A of the colliding nuclei: S+S (A=32) and In+In (A=113) collisions at $p_{\rm lab} = 158A$ GeV/c. Results of the calculations shown in Fig. 4b correspond to monotonous increase of $K_{\rm loss}$ with the mass number of colliding nuclei at high SPS energies. This increase of $K_{\rm loss}$ can be attributed to an increased number of participant nucleons: a probability for secondary inelastic collisions (and thus for the additional energy loss) of participant nucleons evidently increases with N_p.

On the other hand, Figs. 4 and 3 show that at small collision energies $E_{\rm lab} \leq 10$ GeV the inequalities (4) and (5) found from the UrQMD simulations are changed to opposite ones:

$$K_{\rm loss}(p+p) \ > \ K_{\rm loss}(Pb+Pb) \ , \tag{6}$$

$$\left(\frac{\langle\pi\rangle}{\langle N_p\rangle}\right)_{p+p} \ > \ \left(\frac{\langle\pi\rangle}{\langle N_p\rangle}\right)_{Pb+Pb} \ . \tag{7}$$

This happens because of the fusion reactions meson + baryon $\rightarrow$ baryon in dense baryon system created in nucleus-nucleus collisions. As seen from Fig. 3, the change of (7) to (5) is indeed

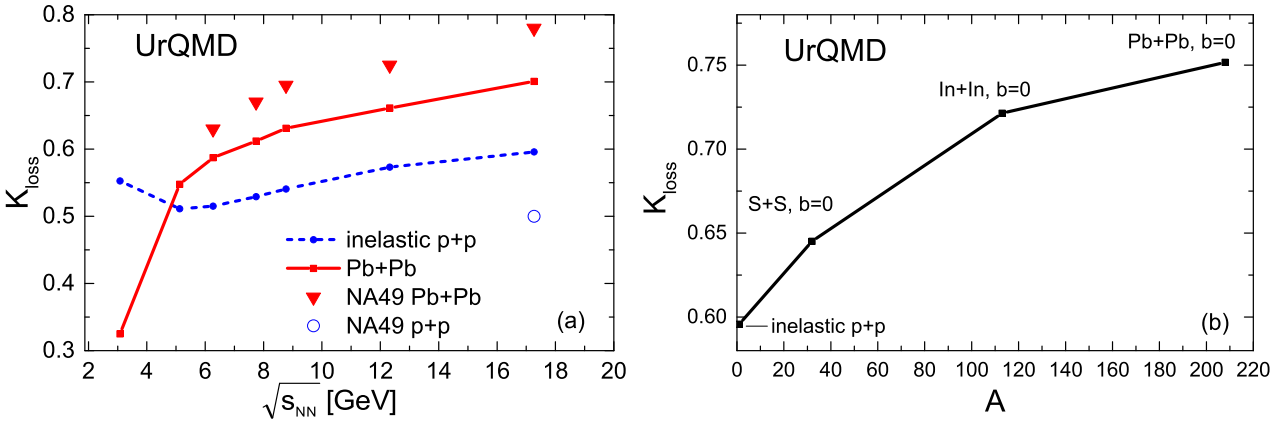

Figure 4: (Color online) The UrQMD results for the quantity $K_{\rm loss}$ (3). (a) The energy dependence in inelastic p+p (the dashed line) and Pb+Pb (the solid line) collisions. Triangular symbols depict the Pb+Pb data and a circle corresponds to the p+p data presented by the NA49 collaboration in Ref. [18] for the inelasticity. (b) The A-dependence for most central (impact parameter $b = 0$) nucleus-nucleus collisions at fixed collision energy of 158A GeV.

observed from the p+p and Pb+Pb data, but at essentially larger collision energy $E_{\rm lab} \geq$ 40A GeV.

IV. PION SPECTRA

A. Rapidity Spectra

The rapidity spectra dN/dy of π^- in inelastic p+p collisions [10] and central Pb+Pb collisions [1, 3] are presented in Fig. 5 for different collision energies. The lines in this figure correspond to the results of the UrQMD simulations. One can see that UrQMD underestimates the total yield of π^- in p+p at all energies except for the highest one, $p_{\rm lab} = 158A$ GeV/c. The deviations are bigger at the mid-rapidity. This fact was also noted in Ref. [19]. Our results for central Pb+Pb collisions are consistent with those published earlier within the UrQMD-2.3 version [20].

As seen from Fig. 5b the UrQMD description of the pion production appears to work much better in central Pb+Pb collisions. This fact looks rather suspicious as the proton-proton results are the input for the UrQMD cascade version description of nucleus-nucleus collisions.

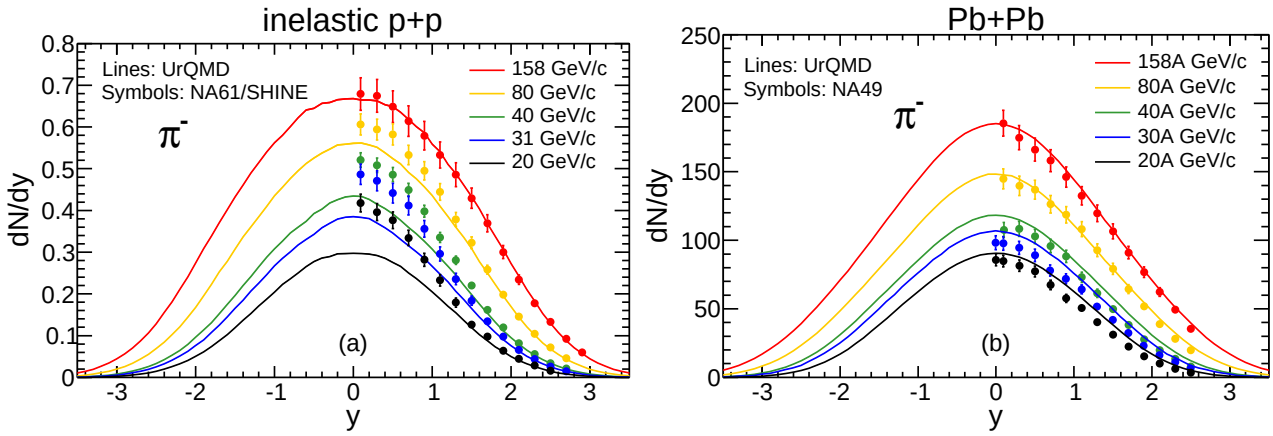

Figure 5: (Color online) The rapidity distributions of π^- in (a) inelastic p+p and (b) central Pb+Pb collisions. The symbols with error bars correspond to the experimental data of NA61/SHINE and NA49 collaborations. The solid lines show the results of the UrQMD calculations.

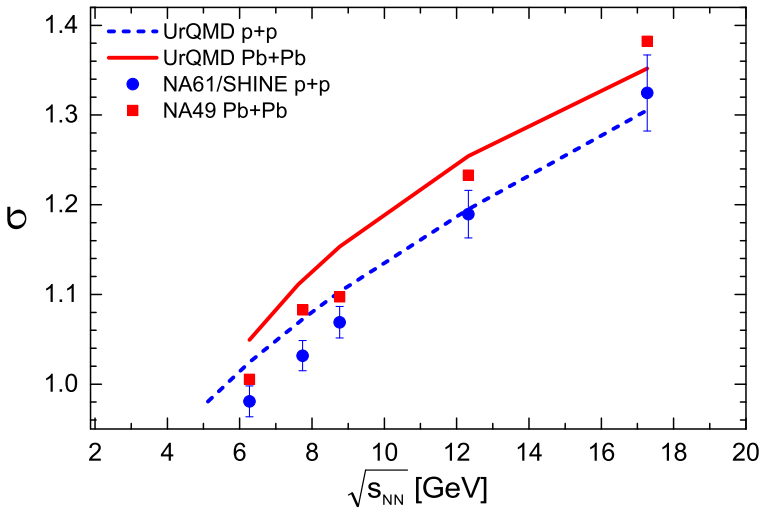

Figure 6: (Color online) The energy dependence of the rapidity width σ for the π^- spectra in inelastic p+p and central Pb+Pb collisions. The data of NA49 and NA61/SHINE collaborations are depicted by symbols while the lines correspond to the UrQMD calculations.

It means that introducing the changes in a theoretical description of the p+p results to achieve an agreement with the NA61/SHINE data [10], one will definitely need to make simultaneously additional changes to preserve the UrQMD agreement with the nucleus-nucleus data.

The width of the rapidity distribution dN/dy is an important feature of the production

process. The width of the rapidity distribution is defined as

$$\sigma \equiv \sqrt{\langle y^2 \rangle - \langle y \rangle^2} \,, \tag{8}$$

where $(k = 1, 2)$

$$\langle y^k \rangle = \frac{\int dy \, y^k \, (dN/dy)}{\int dy \, (dN/dy)} \,. \tag{9}$$

In the center of mass system, $\langle y \rangle = 0$ in a case of the p+p collisions or collisions of identical nuclei. The dependence of the rapidity width σ of the π^- distribution dN/dy on the collision energy in inelastic p+p and central Pb+Pb collisions is shown in Fig. 6. One observes that

$$\sigma(\mathrm{Pb} + \mathrm{Pb}) > \sigma(\mathrm{p} + \mathrm{p}) \tag{10}$$

for the whole SPS energy range. The UrQMD results are in a qualitative agreement with experimental relation (10). However, the UrQMD values of $\sigma(\mathrm{p} + \mathrm{p})$ overestimate the experimental ones at the low SPS energies. This is because of a deficiency of pions in the mid-rapidity region in the UrQMD results seen in Fig. 5a.

Note that the collision energy dependence of the rapidity distribution width for different hadron species in Au+Au collisions was recently studied within the UrQMD approach in Ref. [21].

B. Transverse Mass Distributions

In Fig. 7 the transverse mass distributions of π^- mesons are shown for inelastic p+p (*left*) and central Pb+Pb (*right*) collisions. The symbols with error bars correspond to the experimental data of NA61/SHINE [10] and NA49 [1, 3] collaborations. The data correspond to the mid-rapidity spectra with $0 < y < 0.2$. The solid lines correspond to the UrQMD calculations. In the transverse mass region $0.2 < m_T - m_\pi < 0.7$ GeV/c^2, the spectra for the both p+p and Pb+Pb reactions, and at all collision energies, can be nicely fitted by a simple exponential function

$$\frac{dN}{m_T dm_T} = A \exp\left(-\frac{m_T}{T}\right) \,, \tag{11}$$

where A and T are the fitting parameters, $m_T \equiv \sqrt{p_T^2 + m_\pi^2}$ is the transverse mass with p_T being the pion transverse momentum and m_π the pion mass. The dependence of the inverse

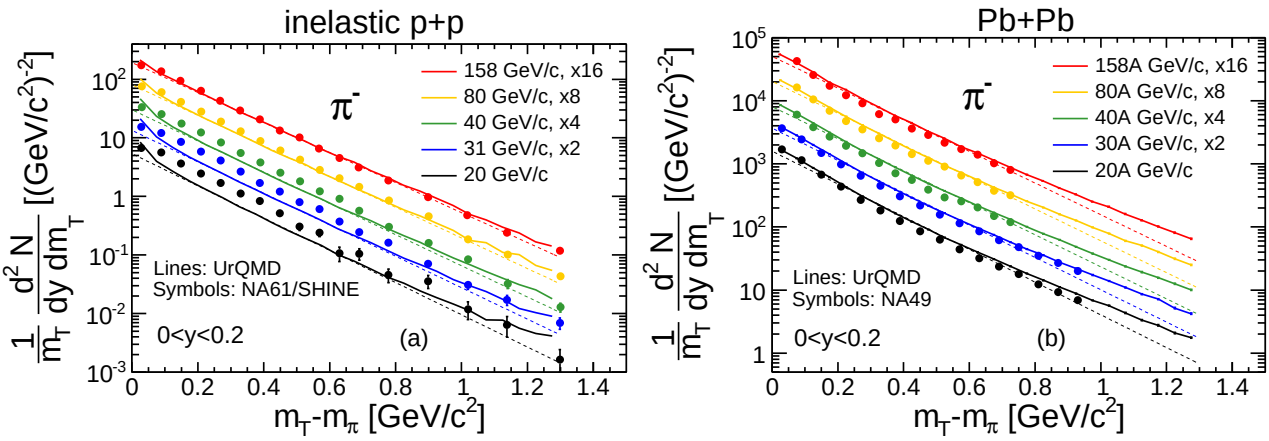

Figure 7: (Color online) The transverse mass distributions of π^- in (a) inelastic p+p and (b) central Pb+Pb collisions. The solid lines correspond to the UrQMD calculations while the symbols with error bars correspond to the experimental data of NA61/SHINE and NA49 collaborations. The dotted lines correspond to the exponential fit (11) of the UrQMD data in the transverse mass interval $0.2 < m_T - m_\pi < 0.7$ GeV/c^2.

slope parameter T of the π^- transverse mass spectra on the collision energy in p+p and Pb+Pb collisions is depicted in Fig. 8a. From this figures one observes that

$$T(\mathrm{p+p}) \ < \ T(\mathrm{Pb+Pb}) \ , \tag{12}$$

for the whole SPS energy range. The UrQMD results are in a qualitative agreement with experimental relation (12). However, UrQMD overestimates systematically the experimental values of the inverse slope T in p+p collisions at all SPS energies.

The inverse slope parameter of the m_T-spectra is dependent on the hadron mass. For inelastic p+p and central Pb+Pb collisions at $p_{\mathrm{lab}} = 158A$ GeV/c this dependence is presented in Fig. 9. The NA49 data [1–3] correspond to the m_T-spectra of π^-, K^-, and p at the mid-rapidity: $0 < y < 0.2$ for π^-, $-0.1 < y < 0.1$ for K^-, and $-0.5 < y < -0.1$ for p. In central Pb+Pb collisions, one observes the following inequalities of the inverse slopes:

$$T_\pi \ < \ T_K \ < \ T_{\mathrm{p}} \ , \tag{13}$$

i.e., rather strong increase of the T parameter with particle mass. In the language of hydrodynamics this increase reflects a presence of the transverse collective flow in nucleus-nucleus

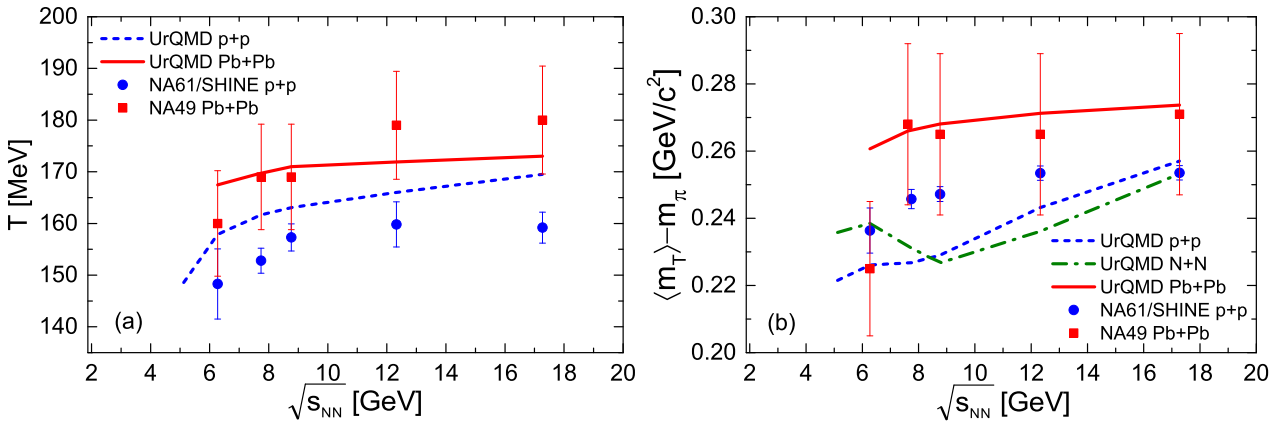

Figure 8: (Color online) The energy dependence of (a) the inverse slope parameter T and (b) the mean transverse mass $\langle m_T \rangle$ of the m_T-spectra of π^- at the mid-rapidity in inelastic p+p and central Pb+Pb collisions. The lines correspond to the UrQMD calculations while the experimental data of NA49 and NA61/SHINE collaborations are depicted by the symbols with error bars.

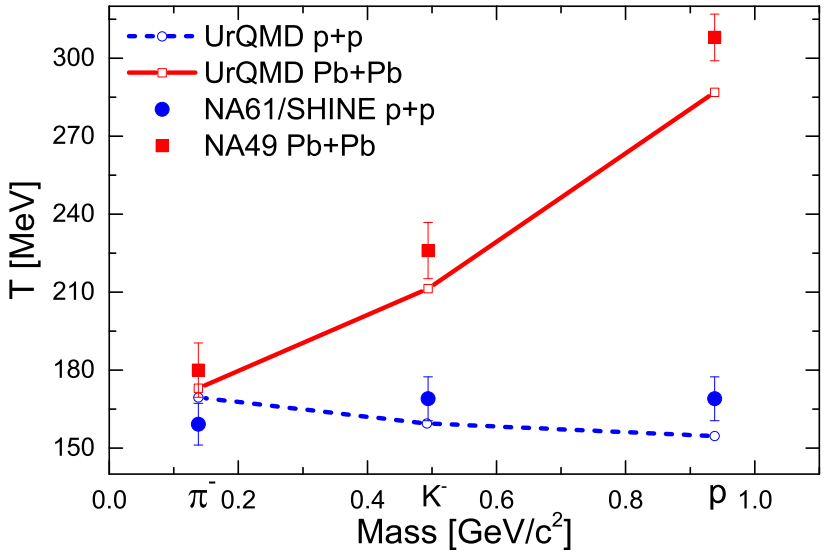

Figure 9: (Color online) Hadron mass dependence of the inverse slope parameter at mid-rapidity in inelastic p+p and central Pb+Pb collisions at $p_{\rm lab} = 158A$ GeV/c. The open symbols correspond to the UrQMD calculations while the data of NA49 [1–3] and preliminary results of NA61/SHINE [22] collaborations are depicted by the full symbols.

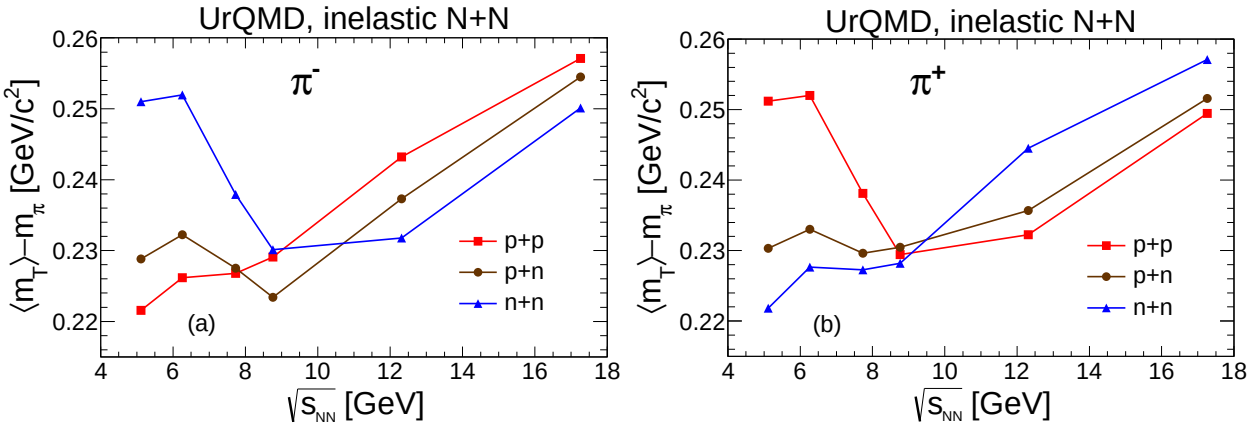

Figure 10: (Color online) The points are the UrQMD results for the mean transverse mass $\langle m_T \rangle$ of (a) π^- and (b) π^+ at mid-rapidity ($0 < y < 0.2$) in inelastic p+p, p+n and n+n. The UrQMD data are depicted by the symbols, and the lines are drawn to guide the eye.

collisions: at the same transverse velocity of the hadronic fluid the particle with larger mass possesses the larger transverse momenta.

The preliminary results of NA61/SHINE [22] correspond to very different behavior in inelastic p+p collisions:

$$T_\pi \cong T_K \cong T_\mathrm{p} \,. \tag{14}$$

Instead of a strong increase of T with hadron mass in Pb+Pb collisions, the value of T is approximately constant for π^-, K^-, and p in p+p collisions.

Next, we investigate a behavior of the mean transverse mass. In Fig. 8b the mean transverse mass of π^- at the mid-rapidity is shown as the function of collision energy in p+p and Pb+Pb collisions. Similar to Eq. (1) one obtains for the mean transverse mass $\langle m_T \rangle$ of π^- or π^+ in nucleon-nucleon collisions:

$$\langle m_T^{NN} \rangle \;=\; \alpha_{pp} \, \langle m_T^{pp} \rangle \;+\; \alpha_{pn} \, \langle m_T^{pn} \rangle \;+\; \alpha_{nn} \, \langle m_T^{nn} \rangle \,, \tag{15}$$

In Fig. 10 the UrQMD results are presented for the mean transverse mass $\langle m_T \rangle$ of π^- (*left*) and π^+ (*right*) at mid-rapidity ($0 < y < 0.2$) in inelastic p+p, p+n, and n+n collisions. One observes a prominent decrease of $\langle m_T \rangle$ for π^- in n+n collisions in the range of laboratory energy between 20 and 40 GeV, and a similar effect for π^+ in p+p collisions. These effects are really important for any analysis of the data in both p+p and A+A collisions.

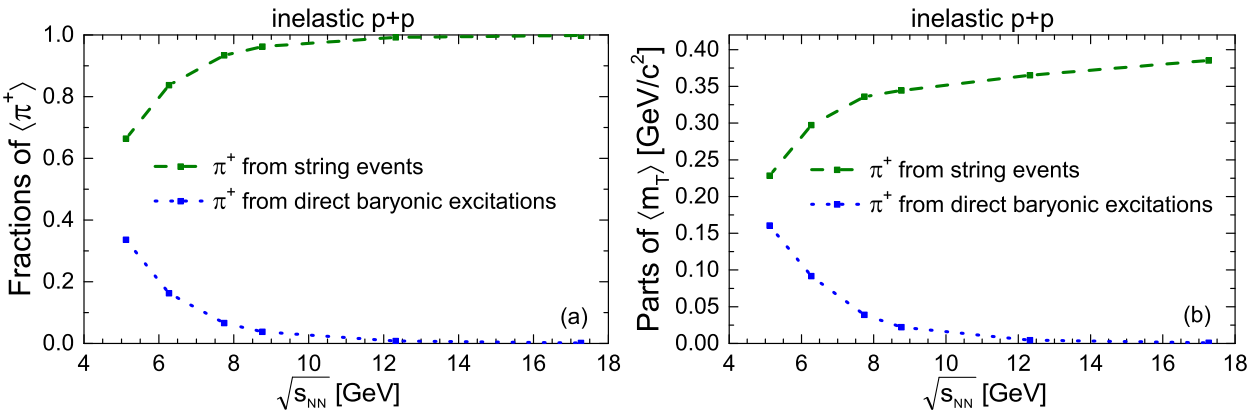

Figure 11: (Color online) The UrQMD results for the π^+ production at the mid-rapidity ($0 < y < 0.2$) in inelastic p+p collisions. The contributions from the two sources of π^+ production are shown: 1) the baryonic resonances produced according to Eq. (16) (the dotted lines); 2) the string produced according to Eq. (17) (the dashed lines). (a) The fractions of the π^+ multiplicity f_B and f_s from the two sources. (b) The parts of the $\langle m_T\rangle$ value $f_B \langle m_T\rangle_B$ and $f_s \langle m_T\rangle_s$ from the two sources.

A physical origin of the non-monotonous energy dependence of $\langle m_T\rangle$ for π^- in n+n collisions and for π^+ in p+p collisions is connected to the presence of two different sources of pion production: excitation and decay of the baryonic resonances N^* and Δ, and excitation and decay of the hadronic strings. In p+p collisions the main inelastic reactions at small energies are the following:

$$p+p \to p+\Delta^+ \,, \quad p+p \to n+\Delta^{++} \,, \quad p+p \to \Delta^+ + \Delta^+ \,, \quad p+p \to \Delta^0 + \Delta^{++} \,,$$
$$p+p \to p+N^+ \,, \quad p+p \to N^+ + \Delta^+ \,, \quad p+p \to N^0 + \Delta^{++} \,. \qquad (16)$$

In the UrQMD simulations, the states N^* with $m = 1440, \ldots, 2250$ MeV and Δ with $m = 1232, \ldots, 1950$ MeV are included [11, 12]. The present version of the UrQMD model includes also the supplementary baryonic resonances N^* and Δ with artificially large masses [23]. Searching for charged pions in the final state, one observes a difference in the production of π^- and π^+: only Δ^0 and N^0 may produce π^-, while other baryonic resonances, Δ^+ and N^+, may produce π^+, and Δ^{++} has to produce π^+, but they can not produce π^-.

Reactions (16) give the dominant contribution to the p+p inelastic cross section at small

collision energies. However, at $\sqrt{s_{NN}} \geq 4$ GeV the excitation of strings,

$$p \ + \ p \ \rightarrow \ \text{string} \ + \ \text{string} \ , \tag{17}$$

opens the new channels of pion production. At $\sqrt{s_{NN}} \geq (6 \div 8)$ GeV the string production dominates in the UrQMD description of the inelastic p+p cross section [11].

In Fig. 11 we present two contributions to the mean multiplicity (*left*) and to mean transverse mass $\langle m_T \rangle$ (*right*) for π^+ at the mid-rapidity, $0 < y < 0.2$, calculated in p+p inelastic collisions within UrQMD simulations: 1) the excitation of baryonic resonances according to Eq. (16) and their decays to π^+ plus nucleon; 2) the excitation of strings according to Eq. (17) and their decays to π^+ plus anything.

The value of $\langle m_T \rangle$ can be presented as

$$\langle m_T \rangle \ = \ f_B \, \langle m_T \rangle_B \ + \ f_s \, \langle m_T \rangle_s \ . \tag{18}$$

In Eq. (18), f_B and f_s correspond to the fractions of π^+ numbers from excited baryons (16) and strings (17), respectively, whereas $\langle m_T \rangle_B$ and $\langle m_T \rangle_s$ are the corresponding values of the mean transverse mass from these two mechanisms. From Fig. 11a one observes that $f_s > f_B$ at all SPS energies, and f_s becomes much larger than f_B with increasing energy. However, at small SPS energies this inequality is partially compensated by the opposite one, $\langle m_T \rangle_B > \langle m_T \rangle_s$. The partial contributions to $\langle m_T \rangle$ coming from baryonic and string decays defined by Eq. (18) are shown in Fig. 11b. The interplay of these two contributions leads to the non-monotonous behavior of their sum $\langle m_T \rangle$ for π^+ in the region $E_{\rm lab} = 20 - 40$ GeV seen in Fig. 10b.

It seems to be also instructive to distinguish three different sources of pion production: all baryonic resonances (including the direct ones produced according to Eq. (16) and those appeared from decays of the strings), all mesonic resonances (appeared from the string fragmentations and from decays of the highly excited baryonic resonances), and the 'direct' pions from string decays (without intermediate resonance states). In Fig. 12 these three contributions calculated within UrQMD in p+p inelastic collisions are presented. The *left* panel (a) shows the fractions of the mean multiplicity and the *right* panel (b) the partial contributions to $\langle m_T \rangle$ value for π^+ at the mid-rapidity, $0 < y < 0.2$. The decrease of $\langle m_T \rangle$ of π^+ with collision energy seen in Fig. 10b appears again as a result of the interplay of these three contributions: a strong

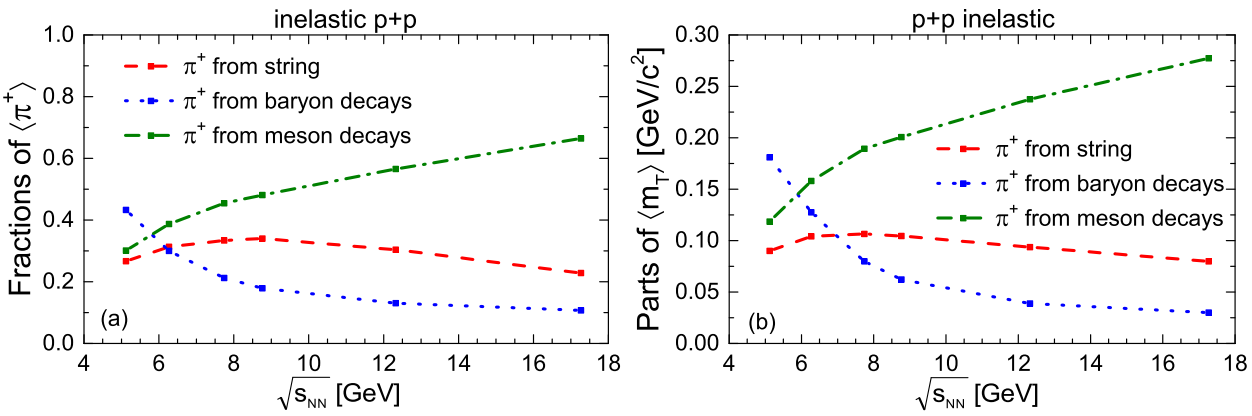

Figure 12: (Color online) The UrQMD results for the π^+ production at the mid-rapidity ($0 < y < 0.2$) in inelastic p+p collisions. The contributions from three sources of the π^+ production are shown: 1) all baryonic resonances (the dotted lines); 2) all mesonic resonances (the dashed-dotted lines); 3) the 'direct' pions from the string decays (the dashed lines). (a) The fractions of the π^+ multiplicity from the three sources. (b) The partial contributions to the $\langle m_T \rangle$ value from the three sources.

decrease with collision energy of the baryonic contribution, an increase of the contribution from the mesonic resonances, and approximately independent of collision energy the contribution of the 'direct' pions from the strings.

Note that our observation of the non-monotonous behavior of $\langle m_T \rangle$ for π^+ with collision energy at $20 < E_{\rm lab} < 40$ GeV in inelastic p+p collisions shown in Fig. 10b is based on the UrQMD results. On the other hand, as it was discussed above, the UrQMD results underestimate the yield of π^- in p+p at $p_{\rm lab} \leq 80$ GeV/c. Therefore, some improvements of the UrQMD model are desirable. As it was mentioned, the present version of the UrQMD code includes many supplementary baryonic resonances N^* and Δ in Eq. (16) with artificially large masses [23]. These resonances influence the UrQMD results for the $\langle m_T \rangle$ of pions at SPS energies. However, a necessity of their presence deserves further studies. It was shown recently in Ref. [19] that an agreement between the UrQMD simulations and the data at the SPS energies can be improved by suppressing the probabilities of binary inelastic reactions (16). Such a modification will lead automatically to the enhanced contribution from the string excitation processes (17). The modified UrQMD code will inevitably change an interplay of the contributions from the baryonic resonances and excited strings.

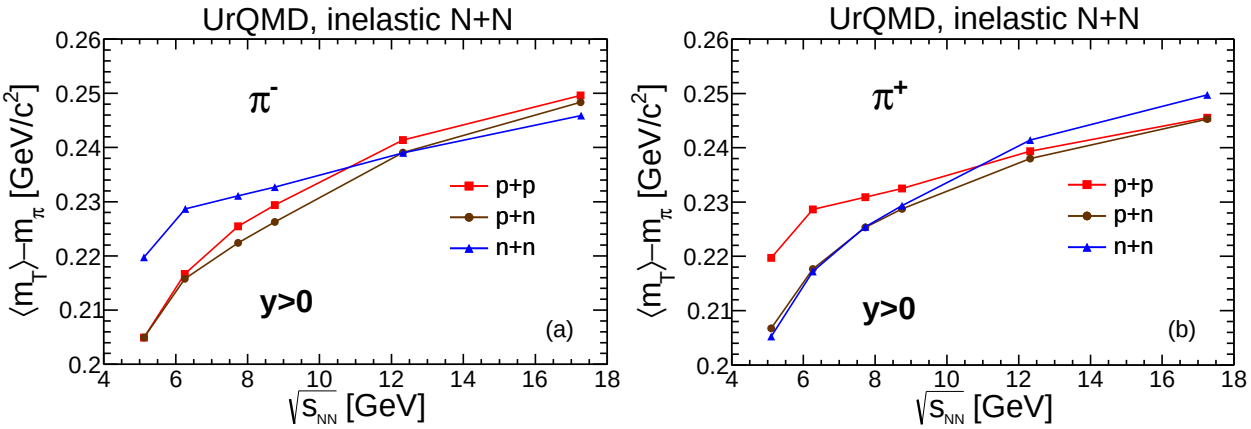

Figure 13: (Color online) The points are the UrQMD results for the mean transverse mass $\langle m_T \rangle$ of (a) π^- and (b) π^+ at all rapidities $y > 0$ in inelastic $p + p$, $p + n$ and $n + n$. The UrQMD data are depicted by the symbols, and the lines are drawn to guide the eye.

Note also that the observed non-monotonous behavior of $\langle m_T \rangle$ is specific for the pions accepted at the mid-rapidity. The UrQMD calculations for all secondary pions presented in Fig. 13 do not show any non-monotonous energy dependence. This is in an agreement with the compilation of old p+p data in Ref. [24]. The dependence of the non-monotonous behavior of $\langle m_T \rangle$ on the size of the rapidity window for the accepted π^+ and other details will be studied further in Ref. [25]. In any case, our UrQMD prediction for the $\langle m_T \rangle$ drop for π^+ at the mid-rapidity at $20 < p_{\rm lab} < 40$ GeV/c in inelastic p+p collisions will be checked soon experimentally by the NA61/SHINE Collaboration.

V. SUMMARY

In the present paper, the UrQMD simulations are exploited for a theoretical modeling of the collision energy and system-size effects for the π^- spectra in inelastic p+p collisions measured recently by the NA61/SHINE [10] and in central Pb+Pb collisions [1–3].

The UrQMD simulations demonstrate that at SPS energies ($E_{\rm lab} \geq 10A$ GeV) each participant nucleon in central nucleus-nucleus collisions transforms more energy to the production of new particles than that in p+p inelastic collisions at the same initial energy per nucleon. At small collision energy $E_{\rm lab} \leq 10A$ GeV the UrQMD simulations show however the opposite be-

havior: the energy loss per participant nucleon $E_{\rm loss}$ becomes larger in inelastic p+p collisions. This UrQMD result is correlated to the inequality between the mean pion multiplicities per participant nucleon, $(\langle\pi\rangle/\langle N_p\rangle)_{p+p}$ and $(\langle\pi\rangle/\langle N_p\rangle)_{Pb+Pb}$. A change of the sign in the difference of the pion multiplicities per nucleon in p+p and Pb+Pb collisions is indeed observed from the data, but at essentially larger collision energy $E_{\rm lab} \cong 40A$ GeV.

The UrQMD results underestimate the total yield of π^- at the mid-rapidity in inelastic p+p collisions at all SPS energies except for the highest one, $p_{\rm lab} = 158A$ GeV/c. The UrQMD description appears to work better in central Pb+Pb collisions. This observation deserves a further analysis. The p+p results are the input for the UrQMD cascade version description of nucleus-nucleus collisions. Thus, any changes of this input, introduced to fit the new p+p data at SPS energies, may destroy an existing agreement with the Pb+Pb data.

The width of the rapidity spectra and the inverse slope of the transverse momentum spectra or the mean transverse mass were investigated on the base of the UrQMD simulations and compared to the data. Both the rapidity width and inverse slope for π^- spectra in Pb+Pb collisions are larger than those in p+p collisions, and for both reactions they increase monotonously with the collision energy. The UrQMD results are in a qualitative agreement with experimental observations.

An important aspect of our analysis is a proper treatment of the isospin effects. They appear to be important for a comparison of the pion production data in proton-proton and nucleus-nucleus collisions. We demonstrate that different results for the pion production in p+p, p+n, and n+n collisions are important not only for π^- and π^+ multiplicities but, even more, for their m_T-spectra. Large difference of about $20-30$ MeV/c^2 in $\langle m_T\rangle$ values for secondary π^- in p+p and n+n inelastic collisions (and the same value with the opposite sign for π^+) is predicted by the UrQMD simulations at low SPS energies, in the energy range corresponding to the future CBM experiment at FAIR. This is important for the analysis of the $\langle m_T\rangle$ dependence on the collision energy in nucleus-nucleus collisions.

The UrQMD simulations predict a non-monotonous behavior of $\langle m_T\rangle$ with collision energy for π^+ in inelastic p+p reactions: the mean transverse mass of positively charged pions accepted at mid-rapidity decreases notably with the collision energy inside the region of $p_{\rm lab} = 20 \div 40$ GeV/c. This our prediction of rather unexpected strong drop of $\langle m_T\rangle$ for π^+ in p+p

collisions will be checked soon by the NA61/SHINE Collaboration.

Acknowledgments

We would like to thank Elena Bratkovskaya, Ivan Kisel, Tobiasz Czopowicz, Marek Gaździcki, Pasi Huovinen, Szymon Pulawski, and Yurij Sinyukov for fruitful discussions and comments. The work of D.V.A. and M.I.G. was supported by the Program of Fundamental Research of the Department of Physics and Astronomy of NAS and by the State Agency of Science, Innovations and Informatization of Ukraine contract F58/384-2013.

---

[1] S.V. Afanasiev *et al.* [NA49 collaboration], Phys. Rev. C **66**, 054902 (2002).

[2] C. Alt *et al.* [NA49 collaboration], Phys. Rev. C **73**, 044910 (2006).

[3] C. Alt *et al.* [NA49 collaboration], Phys. Rev. C **77**, 024903 (2008).

[4] M. Gazdzicki and M. I. Gorenstein, Acta Phys. Polon. **B30**, 2705 (1999);
M. Gazdzicki, M. I. Gorenstein, and P. Seyboth, Acta Phys. Polon. **B42**, 307 (2011), Int. Journ. Mod. Phys. E **23**, 1430008 (2014).

[5] M. Gaździcki [NA61/SHINE Collaboration], J. Phys. G **36**, 064039 (2009).

[6] N. Abgrall *et al.* [NA61 Collaboration], JINST **9**, P06005 (2014).

[7] G. S. F. Stephans, J. Phys. G **32**, S447 (2006); G. Odyniec, PoS CPOD **2013**, 043 (2013).

[8] B. Friman, C. Hohne, J. Knoll, S. Leupold, J. Randrup, R. Rapp, and P. Senger, Lect. Notes Phys. **814**, 1 (2011).

[9] P. Senger [CBM Collaboration], Cent. Eur. J. Phys., **10**, 1289 (2012); see also http://www.fair-center.eu/for-users/experiments/cbm.html.

[10] N. Abgrall *et al.* [NA61 Collaboration], Eur. Phys. J. C **74**, 2794 (2014).

[11] S.A. Bass *et al.*, Prog. Part. Nucl. Phys. **41**, 255 (1998).

[12] M. Bleicher *et al.*, J. Phys. G **25**, 1859 (1999).

[13] A. Bialas, M. Bleszynski, and W. Czyz, Nucl. Phys. B **111**, 461 (1976).

[14] W. Broniowski and W. Florkowski, Phys. Rev. C **65**, 024905 (2002).

[15] V.P. Konchakovski, M.I. Gorenstein, E.L. Bratkovskaya, and W. Greiner, J. Phys. G **37**, 073101 (2010).

[16] A.I. Golokhvastov, Phys. Atom. Nucl. **64**, 1841 (2001).

[17] M. Gaździcki, M.I. Gorenstein, and St. Mrówczyński, Eur. Phys. J. C **5**, 129 (1998).

[18] H. Ströbele [NA49 Collaboration], PoS CPOD **2009**, 044 (2009) arXiv:0908.2777 [nucl-ex].

[19] V. Uzhinsky, arXiv:1308.0736 [hep-ph] and arXiv:1404.2026 [hep-ph].

[20] M. Mitrovski, T. Schuster, G. Gräf, H. Petersen and M. Bleicher, Phys. Rev. C **79**, 044901 (2009).

[21] K. Dey and B. Bhattacharjee, Phys. Rev. C **89**, 054910 (2014).

[22] S. Pulawski [NA61 Collaboration], PoS(CPOD 2013) 056, Proceedings of 8th International Workshop on Critical Point and Onset of Deconfinement, Napa (USA), 11-15 March, 2013; and S. Pulawski, private communications.

[23] H. Petersen, M. Bleicher, S.A. Bass, and H. Stöcker, arXiv:0805.0567 [hep-ph].

[24] A.M. Rossi *et al.*, Nucl. Phys. B **84**, 269 (1975).

[25] V.Yu. Vovchenko, D.V. Anchishkin, and M.I. Gorenstein, in preparation.